Intravenous administration of 99mTc-HMPAO-labeled human mesenchymal stem cells after stroke: in vivo imaging and biodistribution.

Olivier Detante, Anaïck Moisan, Julien Dimastromatteo, Marie-Jeanne
Richard, Laurent Riou, Emmanuelle Grillon, Emmanuel L. Barbier,
Marie-Dominique Desruet, Florence de Fraipont, Christoph Segebarth, et al.

Intravenous Administration of ^{99m}Tc-HMPAO-Labeled Human Mesenchymal Stem Cells After Stroke: In Vivo Imaging and Biodistribution

Olivier Detante,*†‡ Anaïck Moisan,†§¶ Julien Dimastromatteo,†¶# Marie-Jeanne Richard,†**††‡‡
Laurent Riou,†¶ Emmanuelle Grillon,*† Emmanuel Barbier,*† Marie-Dominique Desruet,*§¶
Florence De Fraipont,†,††‡‡ Christoph Segebarth,*† Assia Jaillard,*†§§ Marc Hommel,†‡¶¶
Catherine Ghezzi,†¶ and Chantal Remy*†

*INSERM, U836, Grenoble Cedex 9, France
†Université Joseph Fourier, Grenoble Cedex 9, France
‡Unité Neuro-Vasculaire, Neurologie, Centre Hospitalier Universitaire de Grenoble, Grenoble Cedex 9, France
§Service de Biophysique et Médecine Nucléaire, Centre Hospitalier Universitaire de Grenoble, Grenoble Cedex 9, France
¶Radiopharmaceutiques Biocliniques, INSERM, U877, Faculté de Médecine, La Tronche, France
#ERAS Labo, Saint Nazaire-les-Eymes, France
**Unité Mixte de Thérapie Cellulaire et Tissulaire, Centre Hospitalier Universitaire de Grenoble, Grenoble Cedex 9, France
††Unité de Cancérologie biologique et biothérapie, Centre Hospitalier Universitaire de Grenoble, Grenoble Cedex 9, France
‡‡INSERM, U823, Institut Albert Bonniot, La Tronche Cedex, France
§§Neuroradiologie/IRM, Centre Hospitalier Universitaire de Grenoble, Grenoble Cedex 9, France
¶¶INSERM U003, Centre d'Investigation Clinique, Centre Hospitalier Universitaire, Grenoble Cedex 9, France

Human mesenchymal stem cells (hMSC) are a promising source for cell therapy after stroke. To deliver these cells, an IV injection appears safer than a local graft. We aimed to assess the whole-body biodistribution of IV-injected ^{99m}Tc-HMPAO-labeled hMSC in normal rats ($n = 9$) and following a right middle cerebral artery occlusion (MCAo, $n = 9$). Whole-body nuclear imaging, isolated organ counting (at 2 and 20 h after injection) and histology were performed. A higher activity was observed in the right damaged hemisphere of the MCAo group [$6.5 \pm 0.9 \times 10^{-3}$ % of injected dose (ID)/g] than in the control group ($3.6 \pm 1.2 \times 10^{-3}$ %ID/g), 20 h after injection. In MCAo rats, right hemisphere activity was higher than that observed in the contralateral hemisphere at 2 h after injection (11.6 ± 2.8 vs. $9.8 \pm 1.7 \times 10^{-3}$ %ID/g). Following an initial hMSC lung accumulation, there was a decrease in pulmonary activity from 2 to 20 h after injection in both groups. The spleen was the only organ in which activity increased between 2 and 20 h. The presence of hMSC was documented in the spleen, liver, lung, and brain following histology. IV-injected hMSC are transiently trapped in the lungs, can be sequestered in the spleen, and are predominantly eliminated by kidneys. After 20 h, more hMSC are found in the ischemic lesion than into the undamaged cerebral tissue. IV delivery of hMSC could be the initial route for a clinical trial of tolerance.

Key words: Human mesenchymal stem cell (hMSC); Stroke; Brain ischemia; Cell transplantation; Biodistribution; Nuclear imaging

INTRODUCTION

Stroke is the leading cause of acquired disability in adults in industrialized countries. Admission to specialized stroke units (25,52) and thrombolysis (43,54) are the only effective strategies for the early treatment of acute ischemic stroke. Unfortunately, the brief time window limits thrombolysis to a small fraction of patients. Thus, an alternative strategy is needed that could be ap-

plied later on after the stroke onset with the aim of enhancing brain plasticity (29,41,45,53). It has recently been shown that this could be achieved by cell transplantation (8,36–38).

Among various cell types, human mesenchymal stem cells (hMSC), derived from bone marrow, offer the advantage of not originating from a tumoral or modified source (28). Moreover, they are poorly immunogenic (1,34,48) and do not lead to the ethical problems associ-

ated with embryonic stem cells. The use of hMSC for cell therapy relies on their capacity to graft and survive for a long time in the tissue of interest (12). Bone marrow-derived hMSC are identified as multipotent progenitor cells that differentiate both into mesenchymal and nonmesenchymal lineages, including neurons and endothelia (56). As such, MSC promote structural and functional repair in several organs, notably in the brain after stroke in rodent models using either the intracerebral (10,14,35), intra-arterial (50), or intravenous (IV) (13, 15,34,39,46,51,57) administration. Despite a potential better efficiency of local delivery (intracerebral route), systemic IV administration appears to be safer and easier than local brain grafting following stroke in the clinical setting as it is less invasive. Intracerebral delivery is limited to small graft sites into large ischemic lesions whereas IV injection allows cell distribution into vascularized and viable areas of the lesion. In humans, the first clinical trial demonstrated that IV delivery of hMSC is feasible and safe after stroke (4).

In experimental studies showing a benefit of hMSC administration following stroke, there are little data reported about the quantity of hMSC localizing in the brain lesion and about cell redistribution and/or elimination from other organs. MSC imaging can provide such data. MSCs have previously been labeled with paramagnetic particles for magnetic resonance imaging (MRI) (23) and organs of interest such as the kidneys, liver (21,26), heart (22,32), or brain (27,30) have been studied in vivo. Unfortunately, MRI has a poor sensitivity and whole-body cell MRI is challenging in experimental conditions.

hMSC radioactive labeling (7) and nuclear imaging are better suited for whole-body biodistribution studies. Because of its short decay time (6 h) and its emission energy well adapted to gamma-cameras, thus ensuring high image quality, ^{99m}Tc is better suited than ^{111}In for short tracking of hMSC in vivo (2,6). ^{99m}Tc is a radioactive agent widely used in clinical practice for scintigraphy in nuclear medicine. Technetium 99m-hexamethylpropylene amine oxime (^{99m}Tc-HMPAO) is a lipophilic complex that is reduced into a hydrophilic complex by a glutathione-dependent mechanism after trapping into the cell (44). It provides a stable labeling for in vivo cell tracking, and many cell types have already been labeled with ^{99m}Tc-HMPAO to study cell biodistribution over periods of up to 24 h. In unconditioned mice, Allers et al. (3) mainly observed lung, liver, and spleen activity 24 h after IV injection of hMSC labeled with ^{99m}Tc-HMPAO. Gao et al. (19) confirmed these results in healthy rats after IV injection of ^{111}In-labeled MSC. The authors observed an early lung activity, which redistributed in the liver, kidneys, spleen, and long bones 48 h after injection. Nuclear cell imaging studies have also

been performed in various pathological conditions such as chronic paraplegia (18) and myocardial infarction (5,32). Briefly, radiolabeled MSC were mainly detected in the lungs, liver, kidney, infarcted myocardium, and spleen following IV injection. A recent human case report used bone marrow mononuclear cells radiolabeled with ^{99m}Tc (17). Nine days after ischemic stroke, these cells were injected intra-arterially. Twenty-four hours later, the labeled cells were observed, using in vivo nuclear imaging, in the damaged brain, liver, and spleen (17). To our knowledge, no study assess the biodistribution of IV-injected radiolabeled hMSC after stroke. These data are however necessary to evaluate the risk of a systemic cell therapy after stroke and/or its therapeutic potential, quantifying the hMSC homing to the ischemic lesion.

Thus, the aim of our study was to evaluate the whole-body biodistribution of ^{99m}Tc-HMPAO-labeled hMSC following IV injection in normal rats and in rats subjected to focal cerebral ischemia.

MATERIALS AND METHODS

All animal procedures conformed strictly to French government guidelines for the use and care of animals (license #380806 for O. Detante). Surgical procedures were conducted under aseptic conditions and every effort was made to reduce animal suffering. Anesthesia was induced by inhalation of 5% isoflurane (Forène, Abbott Laboratory) in 30% O_2 in air and maintained throughout all surgical and imaging procedures with 2–2.5% isoflurane through a facial mask.

hMSC Labeling

The hMSC were isolated from bone marrow aspirate from a healthy donor who gave informed consent. Isolation and culture procedures were conducted in the Cell Therapy Unit (biotherapy team of general clinical research centre, University Hospital of Grenoble), in accordance with good laboratory practices. Cell cultures were performed according to previously described methods (42,48).

For each experiment, approximately 7×10^6 hMSC were incubated for 15 min in 370 MBq of ^{99m}Tc-HMPAO prepared according to the instructions of the manufacturer (Ceretec®, GE Healthcare). The preparation was used within 30 min after reconstitution, as recommended (47). Cells were rinsed twice and resuspended in 1 ml of phosphate-buffered saline (PBS) prior to IV injection. These labeling conditions were chosen according to preliminary in vitro assays (data not shown). Flow cytometry was used to check radiolabeled cell viability using 7-amino-actinomycin D (7-AAD, BD PharMingen) at 24 and 48 h after labeling. Colony forming unit fibroblast (CFU-F) assay was also performed to

evaluate the in vitro proliferation capacity of the labeled hMSC.

Animal Model and Experimental Groups

Eighteen adult Sprague-Dawley rats (Janvier, France) weighing between 250 and 300 g were randomly allocated into two groups: 1) a group that underwent a transient right middle cerebral artery occlusion (MCAo) ($n = 9$); 2) an age-matched control group without cerebral ischemia ($n = 9$).

To perform the MCAo, rectal temperature was maintained at $37.0 \pm 0.5°C$ with a feedback-controlled heating electrical blanket connected to a rectal probe. Focal brain ischemia was induced by intraluminal occlusion of the right MCA (40). Briefly, the right carotid arterial tree was isolated. A cylinder of melted adhesive (length 2 mm, diameter 0.38 mm) attached to a nylon thread (diameter 0.22 mm) was advanced from the lumen of the external carotid artery into the internal carotid artery up to 5 mm after the external skull base. The rats were awakened and tested for spontaneous circling and forelimb flexion during the occlusion period. After 90 min, rats were reanesthetized and the thread was removed.

Brain MRI

MRI (7 T horizontal magnet) was performed to measure the ischemic lesion volume with a T_2 spin echo weighted imaging (T_2WI) (TR/TE = 2500/60 ms, field of view = 30 mm, thickness = 1 mm, matrix = 128×128, two averages) in five rats, 1–3 days after MCAo. Rectal temperature was maintained at $37.0 \pm 0.5°C$ with a feedback-controlled heating water blanket. The whole ischemic lesion was manually delineated on each slice. Lesion volumes were computed by multiplying the number of pixels by pixel surface area and slice thickness.To assess blood–brain barrier permeability 1 week after MCAo, T_2WI and T_1WI (same spatial resolution) before and after an IV injection of gadolinium were performed in four additional rats.

Intravenous Injection of hMSC

^{99m}Tc-hMSC (in 1 ml of PBS) were injected as a slow bolus into the saphenous vein. One week after cerebral ischemia, the MCAo group received an injection of $3.4 \pm 1.2 \times 10^6$ cells (corresponding to an injected activity of 78.8 ± 35.1 MBq). The control group received an injection of $3.2 \pm 1.1 \times 10^6$ cells (76.4 ± 24.7 MBq). The injected dose was within the effective therapeutic dose range for IV grafts (15,34,51).To assess the biodistribution of ^{99m}Tc-HMPAO alone, ^{99m}Tc-HMPAO (81.1 ± 3.6 MBq) alone was injected in four additional rats, 1 week after a right MCAo.No immunosuppressive agents were used in agreement with previous studies (16,34).

Whole-Body Nuclear Imaging

Immediately after radiolabeled hMSC injection, the rats were installed in a cradle. The cradle was placed vertically in front of a dual-head small-animal gamma-camera (gamma-imager, Biospace Lab, Paris, France). The two detectors were asymmetrically positioned so that scintigraphic image acquisition of the upper and lower halves of the animal body could be simultaneously performed by each detector, respectively. Gamma-acquisition software (Biospace Lab) was used for image acquisition. The energy window for ^{99m}Tc was 122–170 keV, and decay correction was automatically applied to image counts recorded in the list mode. Image acquisition lasted for 120 min and began immediately following ^{99m}Tc- hMSC injection in all nine control and nine MCAo animals (initial imaging). A second, 120-min acquisition was initiated 18 h following the IV injection in four control and four MCAo rats (late imaging). These animals were awakened between imaging sessions.

Biodistribution by Isolated Organ Counts

Immediately following completion of the initial scintigraphic image acquisition (i.e., 120 min after ^{99m}Tc-hMSC injection), five control and five MCAo rats were euthanized using a lethal dose of pentobarbital by intracardiac injection under isoflurane anesthesia. The euthanasia of the remaining four control and four MCAo rats was performed immediately following the late image acquisition (20 h after injection). Following euthanasia, samples from the left and right cerebral hemisphere, heart, thyroid, salivary gland, stomach, liver, spleen, kidney, lung, and skeletal (hind limb) muscle were quickly obtained, rinsed in physiological saline, and weighed. Samples of blood and urine were also collected. ^{99m}Tc-hMSC activity was assessed using a gamma-well counter (Cobra II, Packard Instruments) with a 120–160 keV ^{99m}Tc energy window. All tissue counts were corrected for background and decay during the time of counting.

Histology

Samples of lung, spleen, liver, and brain were obtained prior to gamma-well counting from both groups. They were stored at −80°C and cut using a cryostat into 20-μm sections. Transplanted hMSC were identified with a human-specific monoclonal antibody to nuclear antigen (MAB1281; 1/2000; Chemicon, CA, USA). This primary antibody was incubated overnight at 4°C. A fluorescent anti-mouse secondary antibody (1/500; Jackson laboratory, MA, USA) was then applied for 1 h. All cell nuclei were counterstained blue with Hoechst prior to examination under epifluorescent microscopy (Nikon Eclipse E600, Japan). Prior to this study, the histological

methodology was set up on brains that had received an intracerebral hMSC grafts after stroke.

Data Analysis

Image Analysis. Gamma-vision + software (Biospace Lab, Paris, France) was used for examiner-blind analysis of planar images. Regions of interest (ROI) were drawn on the whole brain, lung, and both left and right kidneys. No ROI was drawn on the liver because of possible lung superimposition. ROI activities were expressed as counts per minute per mm (cpm/mm^2). Eighteen-hour decay correction was applied to the ROI quantifications that were performed on late images. Initial and late ROI activities were then normalized towards the injected dose expressed as GBq and therefore expressed as cpm/mm^2/GBq.

Biodistribution Analysis. Organ, blood, and urine activities of ^{99m}Tc-hMSC were expressed as cpm, decay-corrected to the time of injection, and normalized to the tissue weight (g) and to the injected dose also expressed as cpm. For the purpose of clarity, these results, initially expressed as percent of the injected dose per gram of sample weight (%ID/g), were finally expressed as 10^{-3} %ID/g.

Statistical Analysis

All results are expressed as mean ± SD. Between-group comparison of mean values was performed using the unpaired Student *t*-test after checking the homogeneity of variance (Levene's test). Paired *t*-test was used for within-group comparison (left vs. right hemisphere). A value of $p < 0.05$ was considered as significant.

RESULTS

hMSC Labeling

Cultured hMSC expressed CD73, CD90, and CD105 but were CD45$^-$ and CD34$^-$ (data not shown). These cells differentiate into osteoblasts, chondrocytes, and adipocytes as previously described (42).

The efficiency of ^{99m}Tc-HMPAO hMSC labeling (i.e., percentage of radiotracer activity incorporated into cells over the total activity of radiotracer mixed with cells) was 26.7 ± 11.6%. In vitro assays showed that more than 96% of the initial ^{99m}Tc activity remained into viable hMSC 4 h after labeling.

Using flow cytometry with 7-AAD, we observed that the ^{99m}Tc-HMPAO-labeled hMSC viability was 97.9% and 96.1%, respectively, at 24 and 48 h after labeling (compared to ~98% viability of unlabeled cells). Cells were also cultured to evaluate their capacity to form colonies. After 10 days of cell culture, no colony was detected for ^{99m}Tc-HMPAO-labeled hMSC whereas 29% of unlabeled hMSC were able to form colony.

Cerebral Lesion Size by MRI

All rats in MCAo group, awakened over the course of the artery occlusion period (90 min), exhibited neurological deficits as a consequence of the ongoing cerebral ischemia. The control rats had no deficit. In addition, the cerebral lesion (infarcted tissue and edema) was authenticated by MRI, 1–3 days following MCAo. Mean volume was 262.5 ± 193.7 mm^3. The four additional rats that were submitted to MCAo and received gadolinium 1 week later exhibited lesion with a markedly increased blood–brain barrier permeability.

Whole-Body Nuclear Imaging

Immediately after labeling, ^{99m}Tc-HMPAO-labeled hMSC were injected in rats. Each group received the same number of cells (3.4 ± 1.2 × 10^6 cells for the MCAo group; 3.2 ± 1.1 × 10^6 cells for control group) and the same injected radioactivity (78.8 ± 35.1 MBq for MCAo group; 76.4 ± 24.7 MBq for control group). Images in Figure 1 were obtained from most representative rats in each group and are given as an example. Table 1 shows quantitative imaging data (corrected for decay) useful for result comparison.

A trend towards higher activity in the whole brain following ischemia was observed in the MCAo group (23.3 ± 3.5 cpm/mm^2/GBq at 2 h and 8.7 ± 1.8 cpm/mm^2/GBq at 20 h) when compared with control rats (20.3 ± 3.5 cpm/mm^2/GBq at 2 h and 7.9 ± 2.1 cpm/mm^2/GBq at 20 h).

An early and significant lung trapping was observed in all rats as indicated by the initially high pulmonary activity. This phenomenon was transient as the lung activity decreased dramatically between the initial and late imaging sessions (control group, from 2209.9 ± 487.2 to 153.5 ± 75.8 cpm/mm^2/GBq; MCAo group, from 2749.2 ± 544.6 to 231.3 ± 39.6 cpm/mm^2/GBq).

Finally, the route of ^{99m}Tc-hMSC elimination was mostly renal as shown from in vivo planar images. Kidney radioactivity was stable over time. No significant difference was observed between the MCAo and control groups.

Concerning whole-body quantification, we observed that, at 20 h, 27.6 ± 6.6% and 29.5 ± 7% of the 2-h activities are still visualized for control and MCAo groups, respectively.

Biodistribution by Isolated Organ Counts

At 2 h following ^{99m}Tc-hMSC injection, the right damaged hemisphere activity in MCAo rats tended to be higher than in controls (11.6 ± 2.8 × 10^{-3} %ID/g vs. 7.9 ± 2.5 × 10^{-3} %ID/g; $p = 0.059$). A marked difference appeared 20 h after injection (6.5 ± 0.9 × 10^{-3} %ID/g vs. 3.6 ± 1.2 × 10^{-3} %ID/g; $p = 0.010$). One out of 10,000 injected ^{99m}Tc-hMSC migrated to the right damaged
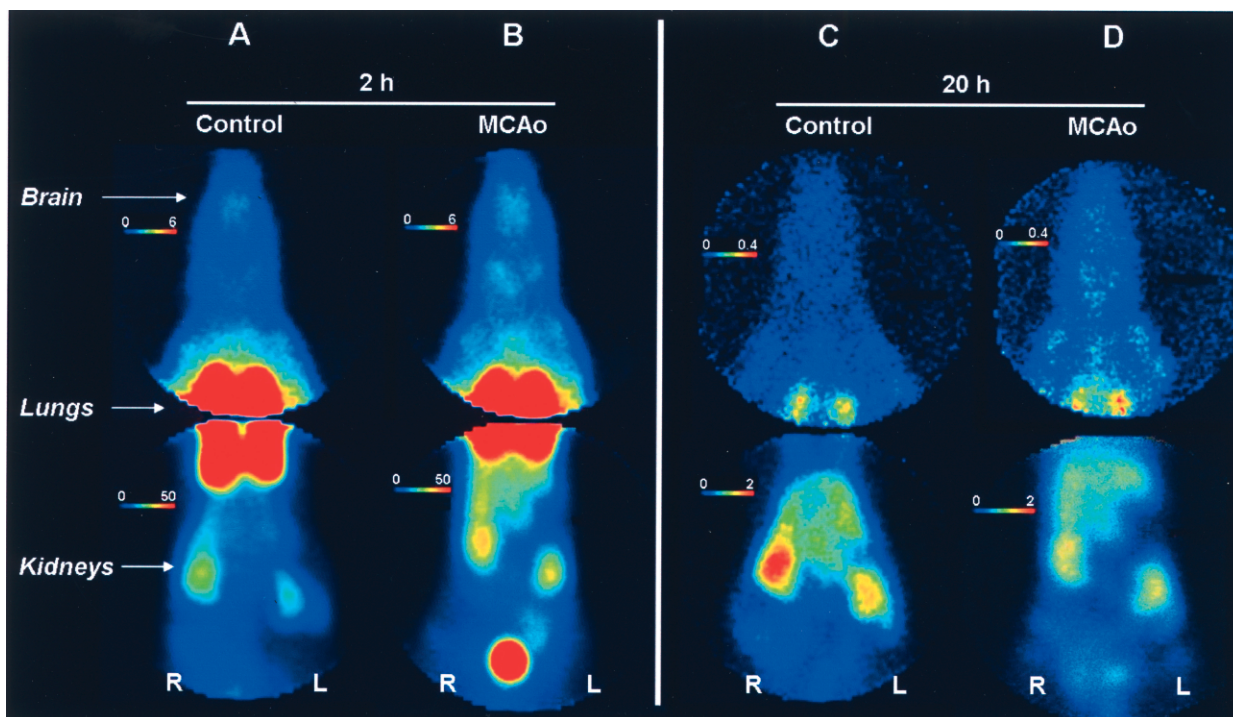
Figure 1. Whole-body nuclear imaging. The two detectors of a small-animal gamma-camera were vertically and asymmetrically positioned. Image acquisition was started immediately following the IV injection of ^{99m}Tc-hMSC for 2 hours (A, B). A second, late planar image was also acquired from 18 to 20 h following the injection (C, D). Regions of interest were drawn on the whole brain, lung, and kidneys. Displayed images were obtained from the most representative rats of each group at each time. Note that the activity scales are different between 2- and 20-h images because of the large difference of activities due to the radioactive decay. L: left; R: right; MCAo: middle cerebral artery occlusion.

hemisphere of MCAo rats. This proportion was half of this in the control rats. Moreover, the late contralateral hemisphere activity was significantly higher in the MCAo group when compared with the control group (Table 2). Within the MCAo group, the initial ipsilateral hemisphere activity was significantly higher than the contralateral one ($11.6 \pm 2.8 \times 10^{-3}$ %ID/g vs. $9.8 \pm 1.7 \times 10^{-3}$ %ID/g, $p = 0.024$) (Fig. 2).

One week after MCAo, IV injection of ^{99m}Tc-HMPAO alone led to higher activity into the left normal hemisphere than in the right damaged one, 2 and 20 h after injection (mean activity right/left hemisphere: 0.93 ± 0.02 and 0.89 ± 0.10, respectively), despite an altered blood–brain barrier in the lesion.

The organ counts indicated that hMSC could colonize an ischemic lesion in the brain after a systemic injection

Table 1. Whole-Body Nuclear Imaging

	0–2 Hours			18–20 Hours		
	Control (n = 9)	MCAo (n = 9)	p	Control (n = 4)	MCAo (n = 4)	p
Brain	**20.3 ± 3.5**	**23.3 ± 3.5**	**ns**	**7.9 ± 2.1 (−62 ± 6%)**	**8.7 ± 1.8 (−65 ± 1%)**	ns
Lung	2209.9 ± 487.2	2749.2 ± 544.6	0.042	153.5 ± 75.8 (−94 ± 3%)	231.3 ± 39.6 (−91 ± 3%)	ns
Right kidney	382.6 ± 151.6	379.4 ± 123.6	ns	353.3 ± 72.2 (+13 ± 28%)	372.4 ± 56.6 (+6 ± 33%)	ns
Left kidney	314.4 ± 101.3	340.4 ± 143.0	ns	310.0 ± 39.8 (+1 ± 21%)	330.3 ± 53.8 (−6 ± 33%)	ns

Two-hour image acquisition was started immediately following the intravenous injection of ^{99m}Tc-hMSC. A second, late planar image was acquired from 18 to 20 h following injection. Results, corrected for decay, are expressed as counts/minute/mm^2/injected GBq (cpm/mm^2/GBq): mean ± SD. Middle cerebral artery occlusion (MCAo) group was compared with control group (unpaired t-test). Percent change (mean ± SD) was calculated per group from values obtained in the four animals that were imaged at 0–2 and at 18–20 h after injection. ns, no significant difference.

**Table 2.** Whole-Body hMSC Biodistribution by Isolated Organ Counting

	2 Hours			20 Hours		
Organ	Control ($n = 5$)	MCAo ($n = 5$)	p	Control ($n = 4$)	MCAo ($n = 4$)	p
Left brain	**7.9 ± 2.5**	**9.8 ± 1.7**	**ns**	**3.6 ± 1.2 (−54%)**	**5.6 ± 0.5 (−43%)**	**0.022**
Right brain	**7.9 ± 2.5**	**11.6 ± 2.8**	**ns (0.059)**	**3.6 ± 1.2 (−54%)**	**6.5 ± 0.9 (−44%)**	**0.010**
Blood	169.9 ± 69.8	145.5 ± 41.4	ns	22.8 ± 4.0 (−87%)	32.0 ± 11.5 (−78%)	ns
Heart	76.3 ± 17.4	103.4 ± 30.5	ns	26.3 ± 3.2 (−66%)	29.1 ± 9.8 (−72%)	ns
Thyroid	34.5 ± 9.9	82.9 ± 52.5	ns	19.4 ± 4.0 (−44%)	24.5 ± 7.5 (−70%)	ns
Salivary gland	43.0 ± 7.7	49.7 ± 24.8	ns	14.2 ± 1.7 (−67%)	20.6 ± 2.6 (−59%)	0.006
Stomach	66.4 ± 21.2	120.4 ± 59.7	ns	25.2 ± 3.0 (−62%)	35.5 ± 20.3 (−71%)	ns
Liver	1363.9 ± 320.0	1508.1 ± 265.4	ns	1011.5 ± 182.2 (−26%)	1311.3 ± 380.6 (−13%)	ns
Spleen	851.9 ± 266.7	796.7 ± 274.1	ns	1434.0 ± 468.3 (+68%)	1825.6 ± 522.8 (+129%)	ns
Kidney	2607.3 ± 661.7	3094.8 ± 657.7	ns	2261.0 ± 438.7 (−13%)	3356.4 ± 165.1 (+8%)	0.003
Lung	18696.0 ± 14675.6	11578.6 ± 11552.6	ns	1181.7 ± 862.7 (−94%)	485.5 ± 241.6 (−96%)	ns
Urine	22479.6 ± 4112.5	27325.4 ± 15781.0	ns	1105.7 ± 732.3 (−95%)	1555.1 ± 1433.3 (−94%)	ns
Muscle	32.8 ± 15.8	27.0 ± 20.4	ns	5.4 ± 1.5 (−84%)	10.2 ± 3.0 (−62%)	0.028

A comparison between control and middle cerebral artery occlusion (MCAo) groups was performed (unpaired t-test). Tracer activity was assessed 2 or 20 h following ^{99m}Tc-hMSC systemic injection and is expressed as percentage of the injected dose per gram of organ (10^{-3} %ID/g): mean ± SD. All tissue counts were corrected for background and decay. Both right (damaged) and left hemisphere were counted for the MCAo group whereas whole brain activity was assessed for the control group. Percent change was calculated per group from mean values obtained across the five animals that were sacrificed at 2 h and across the four that were sacrificed at 20 h after injection. ns, no significant difference.

despite initial cell entrapment in the lungs. Lung trapping was observed on in vivo images and was confirmed by the isolated organ count. Delayed hMSC redistribution then occurred as observed following isolated lung counts in both groups (control group, from 18,696.0 ± 14,675.6 × 10^{-3} %ID/g at 2 h after injection to 1,181.7 ± 862.7 × 10^{-3} %ID/g at 20 h; MCAo group, from 11,578.6 ± 11,552.6 × 10^{-3} %ID/g to 485.5 ± 241.6 × 10^{-3} %ID/g). The IV injection of ^{99m}Tc-HMPAO alone after MCAo led to a much smaller lung activity at both observation time points (2,340.7 ± 180.7 × 10^{-3} %ID/g at 2 h after injection and 1,213.9 ± 468.1 × 10^{-3} %ID/g at 20 h).

Isolated organ counts also confirmed that the kidneys
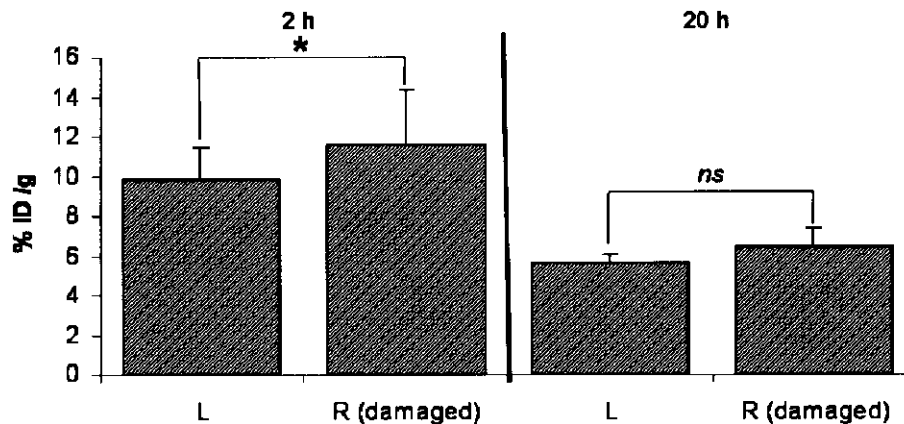
Figure 2. Cerebral distribution of IV injected ^{99m}Tc-hMSC after ischemic lesion shown by gamma-well counting. A within-group comparison (paired t-test, MCAo group) showed a higher activity in the right (R) damaged hemisphere than in the left (L) one ($p = 0.024$ at 2 h; $p = 0.070$ at 20 h) following hMSC injection. Tracer activity is expressed as percent of the injected dose per gram of organ (10^{-3} %ID/g): mean ± SD.

were predominantly involved in the elimination of ^{99m}Tc-hMSC as indicated by the high renal and urinary activity.

Finally, activity in the spleen increased significantly from 2 to 20 h after injection. Such an increase was in contrast with the overall activity decrease observed in all other evaluated organs. These data suggested that hMSC could be sequestered in the spleen.

We did not observe any correlation between the cerebral lesion size and the cellular uptake in the different organs.

Histology

Epifluorescence microscopy images suggested the presence of human cells in lungs, liver, spleen, and brain (damaged and contralateral hemispheres for MCAo group, and control brain only 20 h following hMSC injection) (Fig. 3). No human nuclei were observed in the brain of control rats 2 h following hMSC IV injection. Technical difficulties to obtain histological data from fragile samples as lungs or damaged brain did not allow a histological cell quantification.
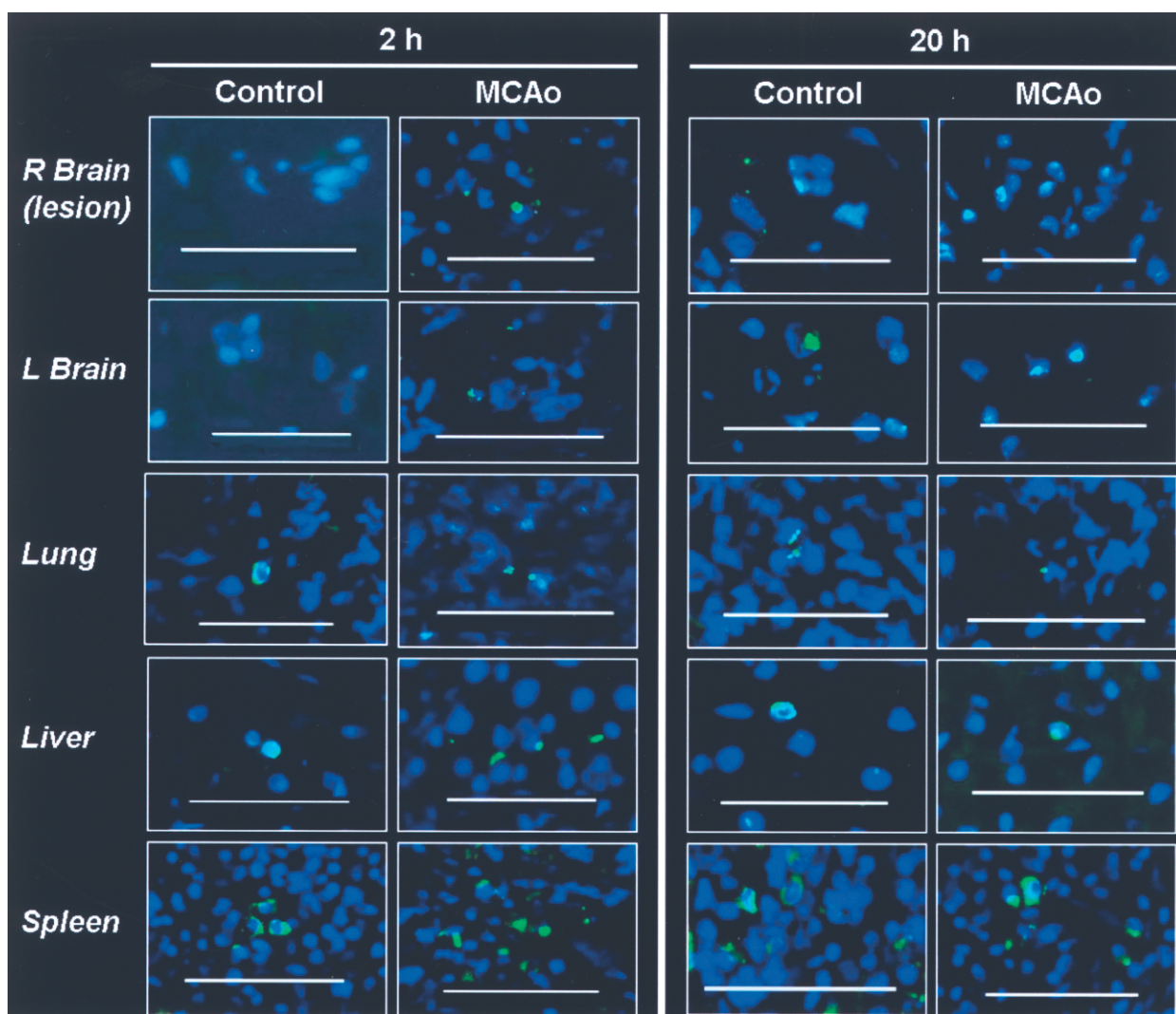
Figure 3. Histology. hMSC were identified as green with a human-specific monoclonal antibody (MAB1281). All cell nuclei were counterstained blue with Hoechst medium. Epifluorescence microscopy merged images showed human cells in lungs, liver, spleen, and brain (in the damaged right hemisphere and the contralateral for MCAo group, and in control brain 20 h following systemic injection of hMSC). No human cells were observed in brains of the control group 2 h after injection. R, right; L, left; MCAo, middle cerebral artery occlusion. Scale bar: 50 μm.

DISCUSSION

Our aim was to evaluate the whole-body biodistribution of IV-injected hMSC after cerebral ischemia. Our results indicate that: 1) some hMSC seems to be able to migrate towards an ischemic brain lesion after a systemic injection despite the initial cell entrapment in the lungs; 2) after 20 h, more hMSC are found in the ischemic lesion than into the undamaged cerebral tissue; 3) hMSC can be sequestered in the spleen and are predominantly eliminated by kidneys; 4) planar nuclear imaging does not reach the sensitivity of gamma-well counting to study the biodistribution of ^{99m}Tc-HMPAO-labeled hMSC.

Cell Labeling and Viability

^{111}In labeling of hMSC at a dose of 30 Bq/cell does not induce cell adverse effects (7), whereas radiation-induced cell damage was observed using ^{111}In labeling of hematopoietic progenitor cells (11). In our experiment, ^{99m}Tc labeling (5 Bq/cell) induces a loss of hMSC ability to form colonies. In vitro, no deleterious effect on cell proliferation was observed with HMPAO alone and loss of hMSC proliferation seems to be due to the radioactive agent (^{99m}Tc) (data not shown). However, our results of flow cytometry with 7-AAD demonstrate a good cell viability over the experimental period (2 days). The alteration of the ability of radiolabeled hMSC to proliferate must be carefully considered as it may alter their therapeutic benefit. For future experiments, especially if related to long-term follow-up as is possible when using ^{111}In labeling, only a small fraction of grafted cells must therefore be radiolabeled and used to track the rest of the unlabeled cell population (17).

IV-Injected hMSC Are Attracted to Cerebral Ischemic Lesion

The apparent hMSC biodistribution within the brain following injection might be due to the release and biodistribution of the ^{99m}Tc-HMPAO. To control this point, we injected ^{99m}Tc-HMPAO alone in rats submitted to MCAo 1 week earlier. Despite an increased blood–brain barrier permeability (observed by MRI), we observed a higher activity in the left normal hemisphere than in the damaged right, 2 and 20 h after injection (mean activity right/left hemisphere = 0.93 ± 0.02 and 0.89 ± 0.10, respectively). The opposite ratios were observed after injection of labeled hMSC (MCAo group: 1.18 ± 0.09 and 1.16 ± 0.10) (Fig. 2). These results suggest that a cell release of ^{99m}Tc-HMPAO would yield an underestimation of the amount of hMSC into the right damaged hemisphere.

Together with isolated brain counting and histology, our results suggest that brain hemispheres, especially the damaged one, may attract viable hMSC following stroke.

Imaging was not able to detect this difference due to a lack of sensitivity. These data about hMSC distribution are in accordance with previously published experimental studies that showed the benefit of IV injected MSC and the survival of grafted cells in the ischemic lesion by histology (13,15,16,57). However, we presently showed that only few injected hMSC are observed in the brain (1/10,000 in the ischemic hemisphere corresponding to 300 cells/3×10^6 injected hMSC). This proportion corresponds to previous histological results that showed a poor graft survival in ischemic brain lesion (1 to 4/10,000) 4 days after IV injection of bone marrow-derived CD133$^+$ cells (9). By histology, Li et al. (34) observed that 4% of 3×10^6 hMSC injected intravenously 24 h after stroke entered the rat brain. In the present study, hMSC were delivered 1 week after stroke and a lower fraction of the injected hMSC was found into the brain. The optimal time of transplantation depends on the desired effect: acute neuroprotection or neuroregeneration in a stabilized lesion (20). Acute hMSC injection after stroke could induce the migration of a bigger number of cells into the damaged tissue. Indeed, most of the chemoattractant agent levels (as cytokines, chemokines, adhesion molecules) are elevated during the first days poststroke and return to baseline in 1 week (20,58). However, an early hMSC injection after stroke is not possible in clinical trials in case of autologous transplantation (culture delay) (4). Our study suggests that, 1 week after stroke, hMSC migrated towards the ischemic brain lesion.

Concerning the whole-body biodistribution, the hMSC homing in nontarget organs such as the spleen that was observed in the present study as well as in others must be carefully considered following either IV (3,19,32) or intra-arterial injection (17).

Graft Route

After IV administration of hMSC, transient early lung trapping was observed in the present study without any obvious respiratory problem. Lung activity then decreased dramatically from 2 to 20 h after injection, suggesting the migration of cells across the lung capillary network. No lung trapping was observed after IV injection of ^{99m}Tc-HMPAO alone. The phenomenon of lung trapping was previously observed in normal rats following IV injection of ^{111}In-labeled MSC, which were detected initially in the lungs and later on in the liver and other organs (19). MSC lung clearance increased following vasodilatation with sodium nitroprusside (19). MSC redistribution from the lungs to nontarget organs (liver, kidney, spleen) and to infarcted myocardium was also observed following IV injection in a canine model (32). All these results suggest transient vascular lung trapping rather than specific MSC homing in the pulmonary tis-

sue. Thus, IV injection of hMSC could be efficiently used despite the initial lung accumulation, which can be reduced using a vasodilatator.

Other graft routes, such as intra-arterial (50) or intra-cerebral delivery, could avoid lung entrapment and thereby increase the number of grafted cells in the target tissue. Intracerebral transplantation of human bone marrow-derived CD133+ cells in rats 1 h and 3 days after stroke resulted in good graft survival (7%) in the transplant site associated with a functional benefit (9). However, IV injection of these cells resulted in poor graft survival (1 to 4/10,000) (9). Lappalaien et al. (33) also showed that ^{111}In labeled neural progenitors can be detected into ischemic hemisphere by nuclear imaging after intra-arterial but not after IV injection. This is consistent with in vivo MRI study showing brain localization of MSC after intra-arterial but not IV injection (55). However, in this study (55), authors reported a clear risk of vascular occlusion after intra-arterial cell delivery according to Doppler flow data. Concerning myocardial infarction, intracoronary stem cell delivery was also found to be more efficient than IV injection (5,24).

Although intra-arterial injection via the carotid artery (17) or intracerebral grafts (31,49) are feasible for treatment of stroke, IV cell injection is less invasive and technically easier than a surgical procedure in the setting of pilot clinical trials (4). Clinical studies using intracerebral grafts in a few patients after stroke reported limited results (31,49). Moreover, the IV injection allows cell distribution into vascularized and viable areas of the lesion and not only into localized graft sites.In the future, more investigations focusing on the peripheral delivery of stem cells are needed to optimize the route and the timing of grafting, and to explain the mechanisms of cell migration towards damaged tissue. Currently phase 2 clinical trials investigating cell therapy tolerance after stroke need to be performed using IV cell injection and additional experimental studies are needed before invasive local delivery is advocated.

CONCLUSION

IV-injected hMSC are transiently trapped in the lungs, can be sequestered in the spleen, and are predominantly eliminated by kidneys. After 20 h, more hMSC are found in the ischemic lesion than into the undamaged cerebral tissue. Thus, IV delivery of hMSC could be the initial route for a clinical trial of tolerance.

REFERENCES

1. Aggarwal, S.; Pittenger, M. F. Human mesenchymal stem cells modulate allogeneic immune cell responses. Blood 105:1815–1822; 2005.

2. Allan, R. A.; Sladen, G. E.; Bassingham, S.; Lazarus, C.; Clarke, S. E.; Fogelman, I. Comparison of simultaneous ^{99m}Tc-hmpao and ^{111}In oxine labelled white cell scans in the assessment of inflammatory bowel disease. Eur. J. Nucl. Med. 20:195–200; 1993.

3. Allers, C.; Sierralta, W. D.; Neubauer, S.; Rivera, F.; Minguell, J. J.; Conget, P. A. Dynamic of distribution of human bone marrow-derived mesenchymal stem cells after transplantation into adult unconditioned mice. Transplantation 78:503–508; 2004.

4. Bang, O. Y.; Lee, J. S.; Lee, P. H.; Lee, G. Autologous mesenchymal stem cell transplantation in stroke patients. Ann. Neurol. 57:874–882; 2005.

5. Barbash, I. M.; Chouraqui, P.; Baron, J.; Feinberg, M. S.; Etzion, S.; Tessone, A.; Miller, L.; Guetta, E.; Zipori, D.; Kedes, L. H.; Kloner, R. A.; Leor, J. Systemic delivery of bone marrow-derived mesenchymal stem cells to the infarcted myocardium: Feasibility, cell migration, and body distribution. Circulation 108:863–868; 2003.

6. Becker, W.; Schomann, E.; Fischbach, W.; Börner, W.; Gruner, K. R. Comparison of [99]Tcm-hmpao and ^{111}In-oxine labelled granulocytes in man: First clinical results. Nucl. Med. Commun. 9:435–447; 1988.

7. Bindslev, L.; Haack-Sorensen, M.; Bisgaard, K.; Kragh, L.; Mortensen, S.; Hesse, B.; Kjaer, A.; Kastrup, J. Labelling of human mesenchymal stem cells with indium-111 for SPECT imaging: Effect on cell proliferation and differentiation. Eur. J. Nucl. Med. Mol. Imaging 33:1171–1177; 2006.

8. Bliss, T.; Guzman, R.; Daadi, M.; Steinberg, G. K. Cell transplantation therapy for stroke. Stroke 38:817–826; 2007.

9. Borlongan, C. V.; Evans, A.; Yu, G.; Hess, D. C. Limitations of intravenous human bone marrow CD133+ cell grafts in stroke rats. Brain Res. 1048:116–122; 2005.

10. Borlongan, C. V.; Lind, J. G.; Dillon-Carter, O.; Yu, G.; Hadman, M.; Cheng, C.; Carroll, J.; Hess, D. C. Bone marrow grafts restore cerebral blood flow and blood brain barrier in stroke rats. Brain Res. 1010:108–116; 2004.

11. Brenner, W.; Aicher, A.; Eckey, T.; Massoudi, S.; Zuhayra, M.; Koehl, U.; Heeschen, C.; Kampen, W. U.; Zeiher, A. M.; Dimmeler, S.; Henze, E. ^{111}In-labeled CD34+ hematopoietic progenitor cells in a rat myocardial infarction model. J. Nucl. Med. 45:512–518; 2004.

12. Chamberlain, G.; Fox, J.; Ashton, B.; Middleton, J. Concise review: Mesenchymal stem cells: Their phenotype, differentiation capacity, immunological features, and potential for homing. Stem Cells 25:2739–2749; 2007.

13. Chen, J.; Li, Y.; Katakowski, M.; Chen, X.; Wang, L.; Lu, D.; Lu, M.; Gautam, S. C.; Chopp, M. Intravenous bone marrow stromal cell therapy reduces apoptosis and promotes endogenous cell proliferation after stroke in female rat. J. Neurosci. Res. 73:778–786; 2003.

14. Chen, J.; Li, Y.; Wang, L.; Lu, M.; Zhang, X.; Chopp, M. Therapeutic benefit of intracerebral transplantation of bone marrow stromal cells after cerebral ischemia in rats. J. Neurol. Sci. 189:49–57; 2001.

15. Chen, J.; Li, Y.; Wang, L.; Zhang, Z.; Lu, D.; Lu, M.; Chopp, M. Therapeutic benefit of intravenous administration of bone marrow stromal cells after cerebral ischemia in rats. Stroke 32:1005–1011; 2001.

16. Chen, J.; Zhang, Z. G.; Li, Y.; Wang, L.; Xu, Y. X.; Gautam, S. C.; Lu, M.; Zhu, Z.; Chopp, M. Intravenous administration of human bone marrow stromal cells induces angiogenesis in the ischemic boundary zone after stroke in rats. Circ. Res. 92:692–699; 2003.

17. Correa, P. L.; Mesquita, C. T.; Felix, R. M.; Azevedo, J. C.; Barbirato, G. B.; Falcão, C. H.; Gonzalez, C.; Mendonça, M. L.; Manfrim, A.; de Freitas, G.; Oliveira, C. C.; Silva, D.; Avila, D.; Borojevic, R.; Alves, S.; Oliveira, A. C. J.; Dohmann, H. F. Assessment of intra-arterial injected autologous bone marrow mononuclear cell distribution by radioactive labeling in acute ischemic stroke. Clin. Nucl. Med. 32:839–841; 2007.

18. De Haro, J.; Zurita, M.; Ayllon, L.; Vaquero, J. Detection of ^{111}In-oxine-labeled bone marrow stromal cells after intravenous or intralesional administration in chronic paraplegic rats. Neurosci. Lett. 377:7–11; 2005.

19. Gao, J.; Dennis, J. E.; Muzic, R. F.; Lundberg, M.; Caplan, A. I. The dynamic in vivo distribution of bone marrow-derived mesenchymal stem cells after infusion. Cells Tissues Organs 169:12–20; 2001.

20. Guzman, R.; Choi, R.; Gera, A.; De Los Angeles, A.; Andres, R. H.; Steinberg, G. K. Intravascular cell replacement therapy for stroke. Neurosurg. Focus 24:E15; 2008.

21. Hauger, O.; Frost, E. E.; van Heeswijk, R.; Deminière, C.; Xue, R.; Delmas, Y.; Combe, C.; Moonen, C. T. W.; Grenier, N.; Bulte, J. W. M. MR evaluation of the glomerular homing of magnetically labeled mesenchymal stem cells in a rat model of nephropathy. Radiology 238:200–210; 2006.

22. Hill, J. M.; Dick, A. J.; Raman, V. K.; Thompson, R. B.; Yu, Z.; Hinds, K. A.; Pessanha, B. S. S.; Guttman, M. A.; Varney, T. R.; Martin, B. J.; Dunbar, C. E.; McVeigh, E. R.; Lederman, R. J. Serial cardiac magnetic resonance imaging of injected mesenchymal stem cells. Circulation 108:1009–1014; 2003.

23. Hinds, K. A.; Hill, J. M.; Shapiro, E. M.; Laukkanen, M. O.; Silva, A. C.; Combs, C. A.; Varney, T. R.; Balaban, R. S.; Koretsky, A. P.; Dunbar, C. E. Highly efficient endosomal labeling of progenitor and stem cells with large magnetic particles allows magnetic resonance imaging of single cells. Blood 102:867–872; 2003.

24. Hofmann, M.; Wollert, K. C.; Meyer, G. P.; Menke, A.; Arseniev, L.; Hertenstein, B.; Ganser, A.; Knapp, W. H.; Drexler, H. Monitoring of bone marrow cell homing into the infarcted human myocardium. Circulation 111:2198–2202; 2005.

25. Indredavik, B.; Bakke, F.; Slordahl, S. A.; Rokseth, R.; Hâheim, L. L. Stroke unit treatment. 10-year follow-up. Stroke 30:1524–1527; 1999.

26. Ittrich, H.; Lange, C.; Togel, F.; Zander, A. R.; Dahnke, H.; Westenfelder, C.; Adam, G.; Nolte-Ernsting, C. In vivo magnetic resonance imaging of iron oxide-labeled, arterially-injected mesenchymal stem cells in kidneys of rats with acute ischemic kidney injury: Detection and monitoring at 3T. J. Magn. Reson. Imaging 25:1179–1191; 2007.

27. Jendelova, P.; Herynek, V.; DeCroos, J.; Glogarova, K.; Andersson, B.; Hajek, M.; Sykova, E. Imaging the fate of implanted bone marrow stromal cells labeled with super-

28. Jiang, Y.; Jahagirdar, B. N.; Reinhardt, R. L.; Schwartz, R. E.; Keene, C. D.; Ortiz-Gonzalez, X. R.; Reyes, M.; Lenvik, T.; Lund, T.; Blackstad, M.; Du, J.; Aldrich, S.; Lisberg, A.; Low, W. C.; Largaespada, D. A.; Verfaillie, C. M. Pluripotency of mesenchymal stem cells derived from adult marrow. Nature 447:880–881; 2007.

29. Jin, K.; Wang, X.; Xie, L.; Mao, X. O.; Zhu, W.; Wang, Y.; Shen, J.; Mao, Y.; Banwait, S.; Greenberg, D. A. Evidence for stroke-induced neurogenesis in the human brain. Proc. Natl. Acad. Sci. USA 103:13198–13202; 2006.

30. Kim, D.; Chun, B.; Kim, Y.; Lee, Y. H.; Park, C.; Jeon, I.; Cheong, C.; Hwang, T.; Chung, H.; Gwag, B. J.; Hong, K. S.; Song, J. In vivo tracking of human mesenchymal stem cells in experimental stroke. Cell Transplant. 16:1007–1012; 2007.

31. Kondziolka, D.; Wechsler, L.; Goldstein, S.; Meltzer, C.; Thulborn, K. R.; Gebel, J.; Jannetta, P.; DeCesare, S.; Elder, E. M.; McGrogan, M.; Reitman, M. A.; Bynum, L. Transplantation of cultured human neuronal cells for patients with stroke. Neurology 55:565–569; 2000.

32. Kraitchman, D. L.; Tatsumi, M.; Gilson, W. D.; Ishimori, T.; Kedziorek, D.; Walczak, P.; Segars, W. P.; Chen, H. H.; Fritzges, D.; Izbudak, I.; Young, R. G.; Marcelino, M.; Pittenger, M. F.; Solaiyappan, M.; Boston, R. C.; Tsui, B. M. W.; Wahl, R. L.; Bulte, J. W. M. Dynamic imaging of allogeneic mesenchymal stem cells trafficking to myocardial infarction. Circulation 112:1451–1461; 2005.

33. Lappalainen, R. S.; Narkilahti, S.; Huhtala, T.; Liimatainen, T.; Suuronen, T.; Närvänen, A.; Suuronen, R.; Hovatta, O.; Jolkkonen, J. The spect imaging shows the accumulation of neural progenitor cells into internal organs after systemic administration in middle cerebral artery occlusion rats. Neurosci. Lett. 440:246–250; 2008.

34. Li, Y.; Chen, J.; Chen, X. G.; Wang, L.; Gautam, S. C.; Xu, Y. X.; Katakowski, M.; Zhang, L. J.; Lu, M.; Janakiraman, N.; Chopp, M. Human marrow stromal cell therapy for stroke in rat: Neurotrophins and functional recovery. Neurology 59:514–523; 2002.

35. Li, Y.; Chopp, M.; Chen, J.; Wang, L.; Gautam, S. C.; Xu, Y. X.; Zhang, Z. Intrastriatal transplantation of bone marrow nonhematopoietic cells improves functional recovery after stroke in adult mice. J. Cereb. Blood Flow Metab. 20:1311–1319; 2000.

36. Lindvall, O.; Kokaia, Z. Recovery and rehabilitation in stroke: stem cells. Stroke 35:2691–2694; 2004.

37. Lindvall, O.; Kokaia, Z. Stem cells for the treatment of neurological disorders. Nature 441:1094–1096; 2006.

38. Lindvall, O.; Kokaia, Z.; Martinez-Serrano, A. Stem cell therapy for human neurodegenerative disorders-how to make it work. Nat. Med. 10(Suppl.):S42–50; 2004.

39. Liu, Z.; Li, Y.; Qu, R.; Shen, L.; Gao, Q.; Zhang, X.; Lu, M.; Savant-Bhonsale, S.; Borneman, J.; Chopp, M. Axonal sprouting into the denervated spinal cord and synaptic and postsynaptic protein expression in the spinal cord after transplantation of bone marrow stromal cell in stroke rats. Brain Res. 1149:172–180; 2007.

40. Longa, E. Z.; Weinstein, P. R.; Carlson, S.; Cummins, R. Reversible middle cerebral artery occlusion without craniectomy in rats. Stroke 20:84–91; 1989.

41. Macas, J.; Nern, C.; Plate, K. H.; Momma, S. Increased generation of neuronal progenitors after ischemic injury in

the aged adult human forebrain. J. Neurosci. 26:13114–13119; 2006.

42. Moriscot, C.; de Fraipont, F.; Richard, M.; Marchand, M.; Savatier, P.; Bosco, D.; Favrot, M.; Benhamou, P. Human bone marrow mesenchymal stem cells can express insulin and key transcription factors of the endocrine pancreas developmental pathway upon genetic and/or microenvironmental manipulation in vitro. Stem Cells 23:594–603; 2005.

43. National institute of neurological disorders and stroke rt-PA stroke study group. Tissue plasminogen activator for acute ischemic stroke. N. Engl. J. Med. 333:1581–1587; 1995.

44. Neirinckx, R. D.; Burke, J. F.; Harrison, R. C.; Forster, A. M.; Andersen, A. R.; Lassen, N. A. The retention mechanism of technetium-99m-hm-pao: Intracellular reaction with glutathione. J. Cereb. Blood Flow Metab. 8:S4–12; 1988.

45. Ohab, J. J.; Fleming, S.; Blesch, A.; Carmichael, S. T. A neurovascular niche for neurogenesis after stroke. J. Neurosci. 26:13007–13016; 2006.

46. Onda, T.; Honmou, O.; Harada, K.; Houkin, K.; Hamada, H.; Kocsis, J. D. Therapeutic benefits by human mesenchymal stem cells (hMSCs) and Ang-1 gene-modified hMSCs after cerebral ischemia. J. Cereb. Blood Flow Metab. 28:329–340; 2008.

47. Piera, C.; Pavía, A.; Bassa, P.; García, J. Preparation of [^{99m}Tc]hm-pao. J. Nucl. Med. 31:127–128; 1990.

48. Plumas, J.; Chaperot, L.; Richard, M.; Molens, J.; Bensa, J.; Favrot, M. Mesenchymal stem cells induce apoptosis of activated t cells. Leukemia 19:1597–1604; 2005.

49. Savitz, S. I.; Dinsmore, J.; Wu, J.; Henderson, G. V.; Stieg, P.; Caplan, L. R. Neurotransplantation of fetal porcine cells in patients with basal ganglia infarcts: A preliminary safety and feasibility study. Cerebrovasc. Dis. 20:101–107; 2005.

50. Shen, L. H.; Li, Y.; Chen, J.; Cui, Y.; Zhang, C.; Kapke, A.; Lu, M.; Savant-Bhonsale, S.; Chopp, M. One-year follow-up after bone marrow stromal cell treatment in middle-aged female rats with stroke. Stroke 38:2150–2156; 2007.

51. Shen, L. H.; Li, Y.; Chen, J.; Zacharek, A.; Gao, Q.; Kapke, A.; Lu, M.; Raginski, K.; Vanguri, P.; Smith, A.; Chopp, M. Therapeutic benefit of bone marrow stromal cells administered 1 month after stroke. J. Cereb. Blood Flow Metab. 27:6–13; 2007.

52. Silvestrelli, G.; Parnetti, L.; Paciaroni, M.; Caso, V.; Corea, F.; Vitali, R.; Capocchi, G.; Agnelli, G. Early admission to stroke unit influences clinical outcome. Eur. J. Neurol. 13:250–255; 2006.

53. Thored, P.; Wood, J.; Arvidsson, A.; Cammenga, J.; Kokaia, Z.; Lindvall, O. Long-term neuroblast migration along blood vessels in an area with transient angiogenesis and increased vascularization after stroke. Stroke 38:3032–3039; 2007.

54. Wahlgren, N.; Ahmed, N.; Dávalos, A.; Ford, G. A.; Grond, M.; Hacke, W.; Hennerici, M. G.; Kaste, M.; Kuelkens, S.; Larrue, V.; Lees, K. R.; Roine, R. O.; Soinne, L.; Toni, D.; Vanhooren, G. Thrombolysis with alteplase for acute ischaemic stroke in the safe implementation of thrombolysis in stroke-monitoring study (sits-most): An observational study. Lancet 369:275–282; 2007.

55. Walczak, P.; Zhang, J.; Gilad, A. A.; Kedziorek, D. A.; Ruiz-Cabello, J.; Young, R. G.; Pittenger, M. F.; van Zijl, P. C. M.; Huang, J.; Bulte, J. W. M. Dual-modality monitoring of targeted intraarterial delivery of mesenchymal stem cells after transient ischemia. Stroke 39:1569–1574; 2008.

56. Woodbury, D.; Schwarz, E. J.; Prockop, D. J.; Black, I. B. Adult rat and human bone marrow stromal cells differentiate into neurons. J. Neurosci. Res. 61:364–370; 2000.

57. Wu, J.; Sun, Z.; Sun, H.; Wu, J.; Weisel, R. D.; Keating, A.; Li, Z.; Feng, Z.; Li, R. Intravenously administered bone marrow cells migrate to damaged brain tissue and improve neural function in ischemic rats. Cell Transplant. 16:993–1005; 2007.

58. Yan, Y.; Sailor, K. A.; Lang, B. T.; Park, S.; Vemuganti, R.; Dempsey, R. J. Monocyte chemoattractant protein-1 plays a critical role in neuroblast migration after focal cerebral ischemia. J. Cereb. Blood Flow Metab. 27:1213–1224; 2007.